HHS Public Access

Author manuscript

J Proteome Res. Author manuscript; available in PMC 2023 February 04.

Published in final edited form as:

J Proteome Res. 2022 February 04; 21(2): 494–506. doi:10.1021/acs.jproteome.1c00865.

Interrogating Kinase–Substrate Relationships with Proximity Labeling and Phosphorylation Enrichment

Tian Zhang,
Department of Cell Biology, Harvard Medical School, Boston, Massachusetts 02115, United States

Anne Fassl,
Department of Cancer Biology, Dana-Farber Cancer Institute, Boston, Massachusetts 02215, United States; Department of Genetics, Harvard Medical School, Boston, Massachusetts 02115, United States

Laura P. Vaites,
Department of Cell Biology, Harvard Medical School, Boston, Massachusetts 02115, United States

Sipei Fu,
Department of Cell Biology, Harvard Medical School, Boston, Massachusetts 02115, United States

Piotr Sicinski,
Department of Cancer Biology, Dana-Farber Cancer Institute, Boston, Massachusetts 02215, United States; Department of Genetics, Harvard Medical School, Boston, Massachusetts 02115, United States

Joao A. Paulo,
Department of Cell Biology, Harvard Medical School, Boston, Massachusetts 02115, United States

Steven P. Gygi
Department of Cell Biology, Harvard Medical School, Boston, Massachusetts 02115, United States

Abstract

Kinases govern many cellular responses through the reversible transfer of a phosphate moiety to their substrates. However, pairing a substrate with a kinase is challenging. In proximity labeling experiments, proteins proximal to a target protein are marked by biotinylation, and mass spectrometry can be used for their identification. Here, we combine ascorbate peroxidase (APEX)

Corresponding Author: **Steven P. Gygi** – *Department of Cell Biology, Harvard Medical School, Boston, Massachusetts 02115, United States*; steven_gygi@hms.harvard.edu.

Supporting Information

The Supporting Information is available free of charge at https://pubs.acs.org/doi/10.1021/acs.jproteome.1c00865.

Complete contact information is available at: https://pubs.acs.org/10.1021/acs.jproteome.1c00865

The authors declare no competing financial interest.

proximity labeling and a phosphorylation enrichment-based workflow, Phospho-APEX (pAPEX), to rapidly identify phosphorylated and biotinylated neighbor proteins which can be considered for candidate substrates. The pAPEX strategy enriches and quantifies differences in proximity for proteins and phosphorylation sites proximal to an APEX2-tagged kinase under the kinase “ON” and kinase “OFF” conditions. As a proof of concept, we identified candidate substrates of MAPK1 in HEK293T and HCT116 cells and candidate substrates of PKA in HEK293T cells. In addition to many known substrates, C15orf39 was identified and confirmed as a novel MAPK1 substrate. In all, we adapted the proximity labeling-based platform to accommodate phosphorylation analysis for kinase substrate identification.

Graphical Abstract

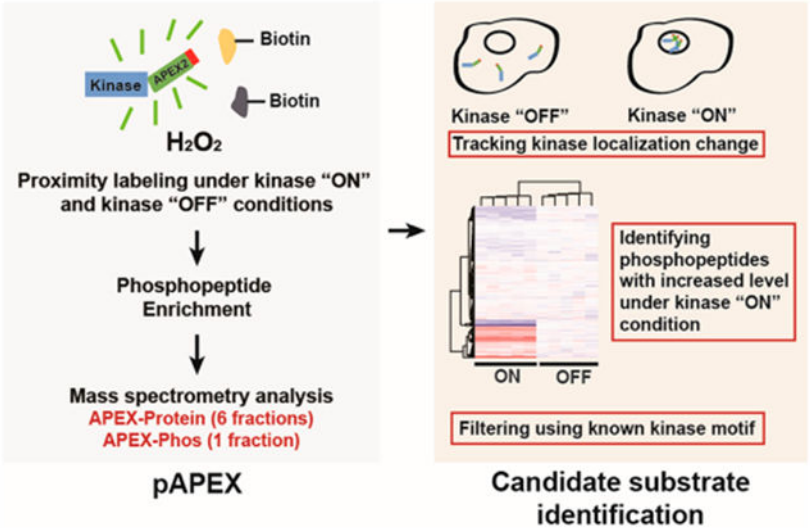

Keywords

proximity labeling; kinases; substrates identification; phosphopeptide enrichment; MAPK1; PKA

INTRODUCTION

The human kinome consists of 518 kinases, including 40 atypical kinases and 478 protein kinases.[1] Protein kinases transfer the γ-phosphate of ATP to a protein,[2] and they regulate important cellular processes including transcription, translation, DNA repair, and signaling transduction.[1] In addition, dysregulated or improper phosphorylation signaling is associated with various diseases.[3–7] The comprehensive identification of kinase substrates represents a grand challenge in proteomics and has the potential to provide clues to both the underlying mechanisms of disease formation as well as accelerating the identification of new therapeutic interventions.

Substrate identification is a major challenge in kinase research. Various methods have been developed for substrate identification.[8] Historically, genetic screening,[9],[10] *in vitro* kinase assays,[11] protein and peptide microassays,[12] and phage display[13] were commonly

used. In addition, KAYAK (Kinase ActivitY Assay for Kinome profiling) was developed to measure the phosphorylation state of dozens of peptides simultaneously and directly using cell lysate.[14] However, phosphorylation *in vitro* may not faithfully represent what occurs in cells. Kinases interact with substrates transiently, making them difficult to be captured by immunoprecipitation.[15] Analogue-sensitive kinases combined with a gamma-thiol ATP analogue have been used to selectively thiophosphorylate targeted substrates.[16] Subsequent LC-MS/MS can identify each labeled substrate. However, the generation of analogue sensitive kinases and the acquisition of enough material are nontrivial, and the generally low abundance of starting material may lead to inconsistent results.[17] Recent developments in mass spectrometry have enabled high throughput screening using phosphoproteome profiling, but it is often not possible to determine if the phosphorylation change is directly or indirectly due to an upstream kinase cascade.[18] In all, a sensitive and robust kinase-substrate identification method with easily interpretable phosphorylation activities is needed.

Ascorbate peroxidase (APEX) proximity labeling maps subcellular proteomes[19,20] including the spatial organization of proteins,[21] RNA,[22] DNA,[23] and metabolites.[24] In a proximity labeling experiment, ascorbate peroxidase catalyzes the transfer of biotin-phenol to its nearby molecules within a small (1–10 nm) radius. It provides a way to enrich for direct phosphorylation events and potentially remove confounding phosphorylation from other kinases by spatial constraint. TMT sample multiplexing enables simultaneous comparison of 10[25] or 16[26,60] samples which can include replicates and all treatments in a single experiment. Enrichment of phosphorylated peptides and mass spectrometry analysis provides localization information for phosphorylation sites. Here, we combined proximity labeling and phosphorylation enrichment to develop a TMT and mass spectrometry-based strategy, Phospho-APEX (pAPEX), for kinase substrate identification.

EXPERIMENTAL PROCEDURES

Plasmid Construction

We created plasmids to express APEX2 tagged MAPK1 in HCT116 and HEK293T cells. Gateway entry clones pDONR223-MAPK1-WT (#82145), pDONAR223-PRKACA (#23495) were purchased from Addgene. pLEX-305 (#41390) lentiviral backbone vector was used and engineered to substitute the hPKG (phosphoglycerate kinase) promoter with the CMV (human cytomegalovirus) promoter plus APEX2 tag fusion with HA tags in the C-terminus of the expression gene. pDONR223_MAPK1_WT were transferred to pLEX305_C-term_APEX2 destination vector using Gateway LR Clonase II enzyme mix (Thermo Fisher) based on the provided protocol. The Gateway cloning product was transformed into One Shot BL21(DE3) chemically competent *E. coli* (Thermo Fisher). Ampicillin was used as the selection marker on the LB plates.

Creation of Stable Cell Lines

HEK293 and HCT116 cells (ATCC) were maintained with DMEM (Gibco) supplemented with 10% FBS (v/v) and 50 U/mL penicillin and 50 U/mL streptomycin (Gibco). One day before transfection, we seeded HEK293T cells at 70% to 90% confluency. Five μg validated clones were combined with viral helper constructs (VSVG, TAT1B, MGPM2, CMV-Rev1B)

at a ratio 4:1 ratio and diluted in 500 μL Opti-MEM with 30 μL P3000 Reagent. Diluted DNA was added to 500 μL Opti-MEM with 22 μL Lipofectamine 3000 reagent. The mixture was incubated at room temperature for 15 min and then added to cells. We then incubated the cells for 3 days for virus production. Virus was collected and filtered using Millex-GP Syringe Filter Unit, 0.45 μm (EMD Millipore). Various amounts of collected virus were added to HEK293T or HCT116 cells. After a 48-h incubation, 2 μg/mL and 0.5 μg/mL puromycin were used for selection of HEK293T and HCT116 cells, respectively. Two days after selection, plates with single clones were continually passaged for further experiments.

Cell Culture and Starvation of the Cells

All cell lines were maintained in DMEM media with 10% FBS and 1% Penicillin–Streptomycin. For the starvation condition, we replaced the cell culture medium 24 h after plating with 10 mL of DMEM supplemented with 1% FBS, and 1% Penicillin–Streptomycin.

Proximity-Based Labeling

After a 24-h starvation, biotinyl tyramide (Toronto Research Chemicals) stock was added directly into starvation media to a final concentration of 500 μM. Cells were incubated in labeling medium for 1 h. EGF or forskolin was added 55 min after media change for a 5 min treatment. An equal amount of PBS buffer was added to the controls. A final concentration of 1 mM hydrogen peroxide was freshly diluted from a 2 M H_2O_2 stock and was added into the medium 59 min after media change to initialize the labeling reaction.

After 1 min of H_2O_2 treatment, cells were washed with ice-cold quenching solution (PBS supplemented with 10 mM sodium ascorbate, 5 mM trolox, and 10 mM sodium azide) three times and quenching solution with 5 mM EDTA once. One mL ice-cold lysis buffer (2 M sodium hydroxide with 7.5% 2-mercaptoethanol in Milli-Q water) was added directly to the plate to harvest the cells. Cell lysates were stored at −80 °C until the next step.

Streptavidin Pull-Down of Biotinylated Proteins

Cell lysates were syringe lysed to fragment DNA (20× with 21-gauge needle), 0.7 mL ice-cold trichloroacetic acid (TCA) was added and the samples were incubated on ice for 15 min. Proteins were precipitated by centrifugation at 21 130*g* at 4 °C for 10 min. Pellets were washed with −20 °C cold acetone, vortexed, and centrifuged at 21 130*g* at 4 °C for 10 min. This step was repeated with ice-cold methanol. Methanol was aspirated and 0.8 mL resuspension buffer (8 M urea, 100 mM sodium phosphate pH 8, 100 mM NH_4HCO_3, 1% SDS (v/v)), was added to the pellets. The pellets were vortexed and suspended in the lysis buffer. A BCA assay determined the protein concentration and an equal amount (2.5–3 mg) of protein was used for each sample for the following steps. Samples were reduced with 5 mM TCEP, alkylated with 10 mM iodoacetamide, and quenched with 15 mM DTT. 50 mM ammonium bicarbonate was added to each sample to reach final concentrations of 4 M urea and 0.5% (v/v) of SDS. A 75 μL suspension equivalent per sample of streptavidin magnetic beads (Thermo Fisher Scientific, stock is at 10 mg/mL, 100 μL can bind 55 μg) were washed twice with 4 M urea, 0.5% SDS (v/v), 100 mM sodium phosphate pH 8, 75 μL of beads were added to each sample, and tubes were rotated for 3 h at room temperature. Following

the streptavidin pull-down, magnetic beads were washed thrice with 4 M urea, 0.5% SDS (v/v), 100 mM sodium phosphate pH 8, once with the 4 M urea, 100 mM sodium phosphate pH 8, and once with 200 mM EPPS pH 8.5 sequentially to remove the SDS in the samples.

On-Beads Digestion and TMT Labeling

Washed beads were resuspended in 100 μL EPPS pH 8.5. 1 μL of LysC stock solution (2 mg/mL, Wako) was added into each sample. Samples were vortexed briefly and incubated at 37 °C for 3 h with shaking. Trypsin (Promega #V51113) was then added at 1:200 (v/v) for further digestion overnight at 37 °C with shaking. Magnetic beads were removed from the samples. Thirty μL acetonitrile were added into each sample. One hundred μg of each TMT 11plex (or TMT 10plex) reagent were used for labeling. After 1 h labeling, 2 μL of each sample were combined, desalted, and analyzed using mass spectrometry. Total intensities were calculated in each channel to determine normalization factors. After quenching using 0.3% hydroxylamine, samples were combined at a 1:1 ratio of peptides based on normalization factors.

Phosphorylated Peptides Enrichment and Off-Line Basic pH Fractionation for pAPEX

High-Select Fe-NTA Phospho-peptide Enrichment Kit (Thermo Fisher) was used to enrich the phospho-peptides according to the manufacturer's protocol. Flow through and washes from phospho-peptide enrichment were combined, dried and fractionated using the High pH Reversed-Phase Peptide Fractionation kit (Pierce). Six fractions were dried, desalted, and analyzed by liquid chromatography-tandem mass spectrometry (LC-MS/MS).

LC-MS/MS Method

The data acquisition method was as described previously.[25] Briefly, for the APEX-Protein fractions, mass spectrometric data were collected on an Orbitrap Fusion Lumos mass spectrometer coupled to a Proxeon NanoLC-1200 UHPLC. The 100 μm capillary column was packed in-house with 35 cm of Accucore 150 resin (2.6 μm, 150 Å; ThermoFisher Scientific). The mobile phase was 5% acetonitrile, 0.125% formic acid (A) and 95% acetonitrile, 0.125% formic acid (B). The data were collected using a DDA-SPS-MS3 method. Each fraction was eluted across a 90 min method with a gradient from 6% to 30% B. Peptides were ionized with a spray voltage of 2600 kV. The instrument method included Orbitrap MS1 scans (resolution of 1.2×10^5; mass range 350–1400 m/z; automatic gain control (AGC) target 1×10^6, max injection time of 50 ms) and ion trap MS2 scans (isolation window: 0.5, CID collision energy of 35%; AGC target 1×10^4; rapid scan mode; max injection time of 60 ms). MS3 precursors were fragmented by HCD and analyzed using the Orbitrap (NCE 65%, AGC 3×10^5, maximum injection time 150 ms, resolution was 50 000 at 400 Th).

Mass spectrometric data for phosphopeptide fractions were collected on an Orbitrap Fusion Lumos mass spectrometer. Mass spectrometric data were collected for each sample using two different synchronous-precursor-selection (SPS)-MS3 methods, one with CID and the second with HCD fragmentation energy at the MS2 stage. The sample was eluted across a 120 min method with a gradient from 6% to 30% B. Peptides were ionized with a spray voltage of 2600 kV. Both instrument methods included Orbitrap MS1 scans (resolution of

1.2×10^5; mass range 350–1400 *m/z;* AGC target 5×10^5, max injection time of 50 ms). The 10 most intense MS1 ions were selected for MS2 analysis. Following acquisition of each MS2 spectrum, a SPS-MS3 scan was collected on the Top 10 most intense ions in the MS2 spectrum. The isolation width was set at 0.4 Da and isolated precursors were fragmented using two methods. In the first method, we used collision induced dissociation (CID) at a normalized collision energy (NCE) of 35% with MultiStage Activation (MSA), and in the second method using higher energy collision-induced dissociation (HCD) at a normalized collision energy (NCE) of 32%. Following acquisition of each MS2 spectrum, a SPS-MS3 scan was collected on the Top 10 most intense fragment ions in the MS2 spectrum. SPS-MS3 precursors were fragmented by higher energy collision-induced dissociation (HCD) at a NCE of 65% and analyzed using the Orbitrap (isolation window: 1.2; mass range 100–2000 *m/z*; AGC target 1.5×10^5; max injection time of 250 ms; resolution was 50 000 at 400 Th). The mass spectrometry proteomics data have been deposited to the ProteomeXchange Consortium via the PRIDE[27] partner repository with the data set identifier PXD028150.

Data Analysis

Mass spectra were processed using a SEQUEST-based software pipeline and searched against the human UniProt database (downloaded on February 14, 2014). Searches were performed using a 50-ppm precursor ion tolerance and 0.9 Da ion tolerance. TMT tags on lysine residues and peptide N termini (+229.163 Da) and carbamidomethylation of cysteine residues (+57.021 Da) were set as static modifications. Oxidation of methionine residues (+15.995 Da) was set as a variable modification. In the phosphopeptide analysis, phosphorylation (+79.966 Da) on serine, threonine, and tyrosine was set as a variable modification. Peptide-spectrum matches (PSMs) were identified, quantified and filtered to a 1% peptide false discovery rate (FDR). In pAPEX protein level analysis, peptides were collapsed to a final protein-level FDR of 1%.

Proteins were quantified by summing reporter ion counts across all matching PSMs. Briefly, a 0.003 Da (3 millidalton) window around the theoretical *m/z* of each reporter ion was scanned and the maximum intensity nearest the theoretical *m/z* was used. For each protein, signal-to-noise (S:N) measurements of the peptides were summed, and these values were normalized to the APEX2 tagged kinase level in each channel. Only proteins with a summed signal-to-noise greater than 100 were used for further analysis. In phosphopeptide analyses, sites with a summed S:N greater than 200 and AScore localization probabilities greater than 13 ($p < 0.05$) were used. The intensities of these sites were normalized using the APEX2 tagged kinase level in each channel derived from pAPEX-Protein analysis. Levels of phosphopeptides pulled down from the same amount of kinase in each channel was used for further analysis.

Immunoprecipitation

HEK293T cells were transduced with lentiviral vectors expressing C-Flag–HA-tagged C15orf39 or C-Flag–HA-tagged GFP. After 48 h of infection, cells were expanded and collected for immuno-precipitation. Three replicates were conducted for each bait. Cells were lysed in 50 mM Tris, pH7.5, 300 mM NaCl and 0.5% NP40 with complete Protease inhibitor cocktail (Sigma) and 1 mM DTT (MCLB buffer). Cell pellets were thawed,

triturated to resuspend and tubes tumbled for 20 min in the cold room (4 °C) to lyse cells. The lysate was spun down at 16.1×10^3 rcf for 20 min at 4 °C to clear lysate. 30 μL 50% anti-HA beads (mouse monoclonal, Sigma) were incubated with cleared lysate for 2–4 h with tumbling at 4 °C. Beads were pelleted by centrifugation for 1 min at 3000 rpm at 4 °C. One mL MCLB buffer was used as wash buffer for a total of 4 washes. One mL PBS was used for washing twice. 100 μL elution buffer (PBS + 250 μg/mL HA peptide (H2N-YPYDVPDYA-COOH (Bio-Synthesis Inc.)) was added into each sample and incubated on a shaker at 37 °C for 30 min. The elution was conducted twice. The two eluates were combined for TCA precipitation. Protein from the TCA precipitation was resuspended in 100 μL 200 mM EPPS for trypsin digestion. Peptides were stage-tipped and analyzed by mass spectrometry.

In Vitro Kinase Assay

C15orf39 was immunoprecipitated using Anti-FLAG M2Magnetic Beads (Sigma-Aldrich) from HEK293T cells overexpressing C-Flag—HA-tagged C15orf39. Beads were resuspended into 40 μL 1× kinase buffer (25 mM MOPS pH 7.2, 1.25 mM glycerol-2-phosphate, 25 mM $MgCl_2$, 5 mM EGTA, 5 mM EDTA, 0.25 mM DTT) and incubated with and without 5 μL human activated ERK2 (MAPK1) (Sigma-Aldrich) and 5 μL 250 μM ATP at 30 °C for 15 min. Beads were then boiled in 1× NuPAGE LDS Sample Buffer (Thermo Fisher) and separated on a NuPAGE 4–12% Bis-Tris Protein Gel (Thermo Fisher). After Coomassie blue staining, gel bands were excised, and protein was extracted for tryptic digestion. Tryptic peptides were analyzed by mass spectrometry.

Confocal Microscopy

HEK293T cells overexpressing C-Flag–HA-tagged C15orf39 (American Type Culture Collection) were plated on glass coverslips. 48 h after infection, cells were fixed with 4% paraformaldehyde for 15 min at room temperature. Cells were washed with PBS, then blocked for 1h with 5% normal goat serum (Cell Signaling Technology) in PBS containing 0.3% Triton X-100 (Sigma). Coverslips were incubated with anti-HA antibodies (mouse monoclonal, clone HA.11, Bio Legend) for 2 h. Cells were washed three times with PBS, then incubated for 1 h with Alexa Fluor-594 conjugated secondary antibodies (Thermo Fisher). Nuclei were stained with Hoechst, and cells were washed three times with PBS and mounted on slides using Prolong Gold mounting media (Thermo Fisher). All images were collected with a Yokogawa CSU-X1 spinning disk confocal scanner with Spectral Applied Research Aurora Borealis modification on a Nikon Ti-E inverted microscope using a 100 × Plan Apo numerical aperture 1.4 objective lens (Nikon Imaging Center, Harvard Medical School). Confocal images were acquired with a Hamamatsu ORCA-AG cooled CCD (charge-coupled device) camera controlled with MetaMorph 7 software (Molecular Devices). Fluorophores were excited using a Spectral Applied Research LMM-5 laser merge module with acousto-optic tunable filter (AOTF)-controlled solid-state lasers (561 nm). A Lumencor SOLA fluorescence light source was used for imaging Hoechst staining. Z series optical sections were collected with a step size of 0.2 μm, using the internal Nikon Ti-E focus motor, and stacked using FIJI (ImageJ) to construct maximum intensity projections.

Immunoblot Analysis and Antibodies

Cells were grown as described above. Cells were collected and syringe lysed in 8 M urea, 200 mM EPPS pH8.5 with cOmplete Protease Inhibitor Cocktail Tablets (Sigma-Aldrich) and Phosphatase Inhibitor Cocktail (Sigma-Aldrich). A BCA assay was performed and 30 μg protein were mixed with NuPAGE LDS Sample buffer (4×) (Thermo Fisher) and denatured. Denatured lysates were separated by NuPAGE 4%–12% Bis-Tris gradient gels (Thermo Fisher) along with Novex Sharp Prestained Protein standard (Thermo Fisher) using MOPS SDS NuPAGE Running Buffer (Thermo Fisher) at 180 V for 55 min. Proteins were transferred to a nitrocellulose membrane using iBlot 2 Transfer Stacks (Thermo Fisher) and an iBlot 2 Gel Transfer Device (Thermo Fisher). The membrane was blocked in 5% milk in TBST at RT for 1 h and incubated in primary antibody in 5% milk in TBST overnight at 4 °C with agitation. Blots were washed thrice for 5 min at RT and then incubated in HRP-conjugated secondary antibody in 5% milk at room temperature (RT) for 1 h. Blots were washed three times as described previously and visualized using SuperSignal West Pico Chemiluminescent HRP Substrate Kit (Thermo Fisher) and Blue Devil Sharp Autoradiography Film (Genesee Scientific).

For the Streptavidin–Biotin IP, beads were eluted using 50 μL 1,1,1,3,3,3-Hexafluoro-2-propanol (Sigma-Aldrich) twice. The eluate was combined, dried, and denatured in loading buffer for Western blotting analysis. After the protein was transferred to the nitrocellulose membrane and blocked in 5% milk in TBST, the membrane was incubated in Streptavidin-HRP conjugate secondary antibody (Invitrogen) in milk for 1 h and then visualized.

RESULTS

pAPEX Enriches Proteins and Phosphorylated Sites in Close Proximity to the APEX2 Tagged MAPK1

To establish the pAPEX method, we used an engineered ascorbate peroxidase with higher catalytic activity (APEX2)[28] and generated an HEK293T cell line stably expressing a well-studied protein kinase, mitogen-activated protein kinase 1 (MAPK1) with an APEX2 and HA tags fusion at the protein's C terminus under expression control by a CMV promoter (Figure 1A). Western blotting analysis confirmed the expression of MAPK1-APEX2 (Figure 1B). A short EGF treatment after serum starvation activates MAPK1 as manifested by higher phosphorylation level.[29] Therefore, we starved the cells in DMEM with 1% FBS for 24 h to create a kinase "OFF" condition and treated serum starved cells for 5 min with 100 ng/mL EGF to create a kinase "ON" condition. A schematic of the proximity procedure under the kinase "ON" condition is shown in Figure 1C. Freshly diluted H_2O_2 was added to the media to a final concentration of 1 mM. During the 1 min of H_2O_2 treatment, APEX2 biotinylated nearby proteins. Immediately afterward, we harvested the cells for Streptavidin–Biotin IP. The kinase "OFF" condition cells were treated in the same way and harvested without EGF treatment (Figure 1C). We next performed a BCA assay, using equal amount of lysate (~3 mg protein) for each Streptavidin–Biotin IP. After the IP, 5% of the beads were analyzed by SDS-PAGE. Ponceau staining and streptavidin-HRP blot showed that Streptavidin–Biotin IP pulled down the same amount of biotinylated protein across the samples (Figure 1D). Then we performed Western blotting to probe phosphorylated canonical MAPK/CDK

substrates motifs, PXS#P or S#PXR/K, in the IP input. The results showed that the level of MAPK/CDK phosphorylated substrate was higher under the “ON” condition in the IP input (Figure 1E), indicating that MAPK was activated and the Streptavidin–Biotin IP enriched phosphorylated proteins in close proximity to the APEX2 tagged MAPK1. These data suggested that MAPK1 fusion with APEX2 can still be activated, and that the kinase “OFF” condition provided an adequate control for the kinase “ON” condition to eliminate nonspecific background of the immunoprecipitation.

pAPEX Experiment Identified Candidate Substrates of MAPK1 in HEK293T Cells

In the pAPEX experiment, we multiplexed five replicates of samples under kinase “ON” and “OFF” conditions, respectively. (Figure 2A). We quantified 3092 proteins in the APEX-Protein analysis (Table S1, Figure 2B). MAPK1 translocates into the nucleus after activation,[30] where it phosphorylates transcription factors[31–33] and structural proteins.[34,35] A previous study showed that the change in localization of an APEX-tagged protein is indicated by changes in its proximal proteins in the proximity labeling experiment.[21] In the pAPEX experiment, we found that many proteins had increased proximity to APEX2-tagged MAPK1 (MAPK1-APEX2) (Figure 2C). Gene ontology (GO) analysis showed that proteins with increased proximity to MAPK1-APEX2 after EGF treatment were enriched in “Nuclear part” (GO:0044428) and other nucleus-related GO categories, while proteins with decreased proximity to MAPK1-APEX2 were mostly enriched in “Cytoplasmic part” (GO:0044444) and “Membrane” (GO:0016020) (Figure 2D). This demonstrates that activated APEX2-tagged MAPK1 translocated to the nucleus and biotinylated nearby proteins. The enrichment of proteins with proximity to MAPK1-APEX2 eliminates indirect substrates by spatial limitation.

We also analyzed phosphorylated peptides from biotinylated proteins using mass spectrometry and quantified 767 sites with AScore localization values >13 ($P < 0.05$) and summed S:N values from 10 channels greater than 200 (Table S2). 591 (90%) of these sites were proline-directed sites (phosphoserine/phosphothreonine-proline). Principle components analysis (PCA) showed EGF treatment separated kinase “ON” and “OFF” conditions and explained 91.0% of the variance (Figure S1A). A heatmap of 767 sites showed the distinct difference of phosphorylation sites between the kinase “ON” and “OFF” states (Figure 2E). Previous studies demonstrated that MAPK1 preferentially phosphorylates serines and threonines that are followed by a proline residue (proline-directed—S/TP).[36] Phosphopeptides with S/TP sites and increased levels under kinase “ON” condition and a Benjamini–Hochberg corrected p-value <0.01 were highlighted in red (Figure 2F). We grouped all the site motifs of 767 phosphorylation sites. 72% (552) of all the phosphorylation sites were found to be within the proline-directed motif, indicating the enrichment of S/TP sites that were in close proximity to the tagged MAPK1 (Figure S1D). Then, we grouped the site motifs of 475 phosphorylation sites with increased levels under the kinase “ON” state (adjusted p-value <0.01). The percentage of phosphorylation sites with proline-directed motif increased to 84% (400) (Figure 2G). We considered all 400 phosphorylation sites as candidate MAPK1 substrates (Table S3) worthy of further validation, while a higher fold increase under kinase “ON” condition served to narrow down the candidate list. In all, pAPEX enriched peptides with a canonical MAPK1

phosphorylation motif and identified candidate kinase substrates of MAPK1 in HEK293T cells.

pAPEX Is Not Specific to HEK293T Cells

We next generated a stable HCT116 cell line expressing APEX2 tagged MAPK1 to further evaluate the pAPEX method in another cell line. Western blotting analysis showed that MAPK1-APEX2 expression levels in HCT116 cells were comparable to that in HEK293T cells (Figure S1B). We then performed a TMT experiment in which we multiplexed five replicates of the kinase "ON" and "OFF" condition. Here, we quantified 3012 proteins (Table S4) and 1499 localized phosphorylation sites (Table S5). PCA using 1499 phosphorylation sites demonstrated that EGF treatment separated the kinase "ON" and kinase "OFF" conditions, explaining 82.7% variance (Figure S1C). A heatmap of normalized phosphorylation sites showed a clear difference between the kinase "ON" and "OFF" conditions (Figure 3A). S/TP sites with the same criteria as Figure 2F were highlighted in red (Figure 3B). All of these 709 phosphorylation sites that had an increased phosphorylation level under the kinase "ON" condition with an adjusted p-value less than 0.01 and within proline-directed motif were considered to be potential MAPK1 substrates in HCT116 cells (Table S6). Among all the potential MAPK1 substrates identified in HEK293T and HCT116 cells, there were many well-studied MAPK1 downstream substrates including NUP153,[20] NUP50,[20] and RBM17.[37] Next, we compared the pAPEX experiments in HEK293T cells and HCT116 cells. APEX-Protein comparison showed that protein changes (ON/OFF) were highly correlated in the two cell lines (Figure 3D) ($r = 0.918$). Then, we compared the phosphorylation changes in APEX-Phos analysis between the two cell lines, which also showed a good correlation ($r = 0.63$) (Figure 3E). Generally, the increases measured under the "ON" condition were higher in HEK293T cells, indicating a stronger response to EGF treatment in HEK293T cells. Examples of overlapping candidate substrates in HCT116 and HEK293T cells are shown in Table 1.

pAPEX Can Identify Candidate Substrates for PKA

We next generated a stable HEK293T cell line expressing APEX2 tagged protein kinase A (PKA) to assess the effect on a different kinase. Forskolin activates the adenylate cyclase enzyme, which generates cAMP from ATP, raising intracellular cAMP levels. cAMP binds and activates PKA.[38] Here, we serum-starved cells overnight to create the kinase "OFF" condition and treated starved cells with 100 μM forskolin for 5 min to create the kinase "ON" condition. We performed a TMT experiment in which we multiplexed five replicates of the kinase "ON" and "OFF" conditions (Figure 4A). 3332 proteins (Table S7) and 823 localized phosphorylated sites (Table S8) were quantified in APEX-Protein and APEX-Phos analyses, respectively (Figure 4B). After forskolin treatment, the intensities of AKAP1,[39] AKAP9[40] and AKAP11[41] decreased dramatically in APEX-Protein, indicating APEX2 tagged PKA dissociated with these anchor proteins after activation[42] (Figure 4C). Activated PKA moved freely and biotinylation increased for nearly all proteins under kinase "ON" condition (Figure 4C). Gene ontology enrichment using all quantified proteins in APEX-Protein identified proteins enriched in many localizations (Figure 4D). A heatmap of the 823 normalized phosphorylation sites showed many sites had elevated phosphorylation level under kinase "ON condition (Fig. 4E). PCA demonstrated that the forskolin treatment

separated the kinase “ON” and kinase “OFF” conditions, explaining 83.4% of the variance (Fig. S1E). It is known that PKA preferentially phosphorylates serine or threonine residues at basic motifs (RXXS/T).[43] We highlighted 184 sites within RXXS/T motif and with an increased phosphorylation level under the kinase “ON” condition and an adjusted *p*-value less than 0.01 (Figure 4F, middle), which were candidate substrates of PKA (Table S9). Many of these sites (51) also contained the full motif (RRXS/T) (Figure 4F, bottom), which is the more stringent PKA substrate motif.[44] Here, pAPEX-PKA identified candidate PKA substrates. Examples of 10 sites with large increases under kinase “ON” condition are listed in Table 2. In all, pAPEX was applied after activating two different kinases.

Examples of Potential Substrates Identified by pAPEX

In pAPEX experiments, we confirmed substrates from previous studies. For example, CTNNB1 S552 is a PKA dependent event, which regulates stem cell differentiation[45] and transcription.[46] PPP2R5D S573 has been indicated to be involved in potential β-adrenergic regulation of PP2A in cardiomyocytes[47] (Table 2). We identified these sites as potential substrates of PKA in pAPEX. Among all the potential substrates identified for MAPK1, TPX2 has also been identified as a substrate using the analogue sensitive (AS) MAPK1.[48] pT369 on TPX2 was elevated under kinase “ON” condition in pAPEX of MAPK1 in both cell lines. A previous study has shown that MAPK phosphorylates the N terminus of the JunD and activates JunD in response to EGF.[49] Phosphorylation of S62 on N-Myc stabilizes N-Myc and regulates cell proliferation via ERK.[50] In addition, S58 on N-Myc can be phosphorylated via GSK-3β.[51] Here, in HCT116 cells, we captured the peptides with pT58 on MYCN and pS90 on JUND through pAPEX (Figure 5A).

Other than these studied substrates, we also identified novel substrates of the tagged kinases in pAPEX. For example, DDX17, probable ATP-dependent RNA helicase, is involved in multiple cellular processes regulating the alternative spicing of exons with specific features.[52,53] To our knowledge, there have been no previous studies focusing on the phosphorylation of DDX17 by MAPK1. Here, we identified DDX17 as a candidate substrate in both HCT116 and HEK293T cells (Figure 5A, Table 1). As such, further study of how MAPK1 regulating RNA splicing by phosphorylating DDX17 may provide a novel regulating mechanism of MAPK1.

During the preparation of this manuscript, a report of candidate substrates using PKA fused with BioID appeared with a 24-h labeling.[54] Four out of 35 candidate substrates from that paper were identified in our study.

We also identified C15orf39 (pS364) as a novel candidate substrate of MAPK1 in both HEK293T and HCT116 cells. In the pAPEX experiment, the phosphopeptide levels associated with pS364 on C15orf39 increased after EGF treatment (Figure 4A, Table 1). C15orf39 is an uncharacterized protein. To explore the localization of C15orf39, we created an HEK293T cell line stably expressing C-Flag–HA-tagged C15orf39 and performed HA immunostaining. HA and Hoechst staining overlapped in the nucleus of HEK293T cells, indicating that C15orf39 is localized to the nucleus (Figure 5B). Bioplex interactome data showed that MAD2L1 is a shared interactor in HEK293T and HCT116 cells.[55] We repeated the immunoprecipitation of C-Flag–HA-tagged C15orf39 in HEK293T cells and analyzed

the captured proteins by mass spectrometry. The results confirmed that MAD2L1 is an interactor of C15orf39 in HEK293T cells (Figure 5C). MAD2L1 is a component of the spindle assembly checkpoint and is required for mitotic check.[56–58] On the basis of these data, we hypothesized that C15orf39 has a cellular role that might be manifest in mitosis and cell proliferation through its interaction with MAD2L1. To confirm that C15orf39 is a substrate of MAPK1, we performed a mass spectrometry-based *in vitro* kinase assay using purified active MAPK1 and C15orf39. The Skyline application was used to visualize the base peak of the peptides harboring pT364 from C15orf39 and their corresponding nonphosphorylated versions (Figure 5D). The levels of the nonphosphorylated peptide (LEPPLTPR) appeared to decrease and the levels of the phosphorylated version of that peptide (LEPPLpTPR) increased after incubation with MAPK1. These *in vitro* kinase assay results confirm that pS364 in C15orf39 can be phosphorylated by MAPK1.

DISCUSSION

Reversible protein phosphorylation is a foundational principle that is integral to numerous cellular processes and diseases. Understanding kinase–substrate relationships is a long-standing challenge in proteomics and new technologies are needed to help assign substrates to kinases. Proximity labeling of kinases facilitates the biotinylation of nearby proteins which would include substrates. The goal of this study was to identify phosphorylated substrates of kinases by proximity labeling. We termed this technique pAPEX for phospho-APEX. In this strategy, the kinase is interrogated for phosphorylated neighbors under two conditions-kinase “ON” and kinase “OFF.” In this way, changes in the levels of phosphorylated peptides between these two states can be used to create lists of potential substrates. We demonstrated the technique first with MAPK1 (Erk2 kinase) and then using PKA. In both cases, phosphorylated peptides with differential abundance were used to identify potential substrates matching the known kinases phosphorylation motif.

pAPEX relies on isobaric tagging with TMT for sample multiplexing and phosphopeptide quantification.[59,60] TMT-based experiments allow for complex experimental designs where multiple conditions and multiple replicates are included in the same experiment. In this case, we used 10-plex reagents that allowed for two conditions (“ON” and “OFF”) each with five biological replicates to be simultaneously quantified in the same experiment.

Proximity labeling as described here can reveal localization or conformational changes after kinase activation. For MAPK1, a 5 min activation using EGF resulted in a clear shift of the protein to the nucleus (Figure 2C). PKA, however, after 5 min activation with forskolin resulted in increased biotinylation for several thousand proteins (Figure 4C). PKA in the unstimulated state has the catalytic subunit bound in a tetrameric complex with 2 copies of each of the regulatory and catalytic subunits.[42] Under these conditions, we postulate that the biotinylation events are not as efficient. Upon stimulation, the catalytic subunit is released and is free to interact with its environment where the APEX tag would encounter a much larger number of proteins. Despite the dynamic changes in the biotinylation of nearby proteins, candidate substrates for these kinases were still be identified based on (i) the increase in abundance of the phosphopeptide and (ii) the filtering of sites for known kinase motifs.

The results of both the MAPK1 and PKApAPEX experiments confirmed many known substrates and provided additional unknown candidates that contained each kinase's consensus phosphorylation sequence and demonstrated increased phosphorylation under the "ON" conditions. For example, for MAPK1, we confirmed that pS364 of an uncharacterized protein termed C15orf39 can, indeed, be phosphorylated by MAPK1 through an *in vitro* kinase assay. Further explorations of the role of this site and the function of this protein are underway.

Notably, hydrogen peroxide, which was used in pAPEX experiments, enhances protein tyrosine phosphorylation by activating protein tyrosine kinases while inactivating protein tyrosine phosphatases,[61] which may limit the use of pAPEX on tyrosine kinases for substrate identification. Though pAPEX provides spatial constraint to limit the indirect phosphorylation events being pulled down and analyzed, further confirmation assays, such as an *in vitro* kinase assay, should be performed to confirm candidate substrates for further investigation.

In conclusion, we adapted the APEX2 proximity labeling strategy toward the identification of potential substrates of kinases. pAPEX tracks the kinase phosphorylation process, helps to reduce indirect kinase substrates, and increases the sensitivity for high-throughput studies of kinase substrates. In the future, pAPEX could be combined with analogue-sensitive kinases[62] and other advanced mass spectrometry methods, such as TMT-18plex[59] and FAIMS,[63] and make use of real-time analytics[64] to improve substrate detection and uncover the mechanisms governing the cellular roles of many kinases.

Supplementary Material

Refer to Web version on PubMed Central for supplementary material.

ACKNOWLEDGMENTS

We thank the Nikon Imaging Center at Harvard Medical School for use of the spinning disk confocal microscope. We thank the members of the Gygi lab at Harvard Medical School for exciting discussions. This work was funded in part by NIH grants GM132129 (J.A.P.) and GM067945 (S.P.G.).

REFERENCES

(1). Manning G; Whyte DB; Martinez R; Hunter T; Sudarsanam S The Protein Kinase Complement of the Human Genome. Science 2002, 298, 1912. [PubMed: 12471243]

(2). Wang Z; Cole PA Catalytic mechanisms and regulation of protein kinases. Methods Enzymol 2014, 548, 1–21. [PubMed: 25399640]

(3). Grundke-Iqbal I; et al. Abnormal phosphorylation of the microtubule-associated protein tau (tau) in Alzheimer cytoskeletal pathology. Proc. Natl. Acad. Sci. U. S. A 1986, 83, 4913–4917. [PubMed: 3088567]

(4). Lahiry P; Torkamani A; Schork NJ; Hegele RA Kinase mutations in human disease: interpreting genotype-phenotype relationships. Nat. Rev. Genet 2010, 11, 60–74. [PubMed: 20019687]

(5). Bhullar KS; Lagaron NO; McGowan EM; Parmar I; Jha A; Hubbard BP; Rupasinghe HPV. Kinase-targeted cancer therapies: progress, challenges and future directions. Mol. Cancer 2018, 17,48–48. [PubMed: 29455673]

(6). Alessi DR; Sammler E LRRK2 kinase in Parkinson's disease. Science 2018, 360, 36. [PubMed: 29622645]

(7). Fountas A; Diamantopoulos LN; Tsatsoulis A Tyrosine Kinase Inhibitors and Diabetes: A Novel Treatment Paradigm? Trends Endocrinol Metab 2015, 26, 643–656. [PubMed: 26492832]

(8). Johnson SA; Hunter T Kinomics: methods for deciphering the kinome. Nat. Methods 2005, 2, 17–25. [PubMed: 15789031]

(9). Paradis S; Ruvkun G Caenorhabditis elegans Akt/PKB transduces insulin receptor-like signals from AGE-1 PI3 kinase to the DAF-16 transcription factor. Genes Dev. 1998, 12, 2488–2498. [PubMed: 9716402]

(10). Clark IE; et al. Drosophila pink1 is required for mitochondrial function and interacts genetically with parkin. Nature 2006, 441, 1162–1166. [PubMed: 16672981]

(11). Delom F; Chevet E Phosphoprotein analysis: from proteins to proteomes. Proteome Science 2006, 4, 15. [PubMed: 16854217]

(12). Zhu H; et al. Global Analysis of Protein Activities Using Proteome Chips. Science 2001, 293, 2101. [PubMed: 11474067]

(13). Fukunaga R; Hunter T MNK1, a new MAP kinase-activated protein kinase, isolated by a novel expression screening method for identifying protein kinase substrates. EMBO J. 1997, 16, 1921–1933. [PubMed: 9155018]

(14). Kubota K; et al. Sensitive multiplexed analysis of kinase activities and activity-based kinase identification. Nat. Biotechnol 2009, 27, 933–940. [PubMed: 19801977]

(15). Smith MG; Ptacek J; Snyder M In Protein Microarray for Disease Analysis: Methods and Protocols; Wu CJ, Ed.; Humana Press: Totowa, NJ, 2011; pp 201–212.

(16). Koch A; Hauf S Strategies for the identification of kinase substrates using analog-sensitive kinases. Eur. J. Cell Biol 2010, 89, 184–193. [PubMed: 20061049]

(17). Lopez MS; Kliegman JI; Shokat KM In Methods in Enzymology; Shokat KM, Ed.; Academic Press, 2014; Vol. 548, pp 189–213. [PubMed: 25399647]

(18). Riley NM; Coon JJ Phosphoproteomics in the Age of Rapid and Deep Proteome Profiling. Anal. Chem 2016, 88, 74–94. [PubMed: 26539879]

(19). Eisenstein M Marked for depth. Nat. Methods 2013, 10, 284–284. [PubMed: 23653924]

(20). Kosako H; et al. Phosphoproteomics reveals new ERK MAP kinase targets and links ERK to nucleoporin-mediated nuclear transport. Nature Structural & Molecular Biology 2009, 16, 1026–1035.

(21). Paek J; et al. Multidimensional Tracking of GPCR Signaling via Peroxidase-Catalyzed Proximity Labeling. Cell 2017, 169, 338–349. [PubMed: 28388415]

(22). Kaewsapsak P; Shechner DM; Mallard W; Rinn JL; Ting AY Live-cell mapping of organelle-associated RNAs via proximity biotinylation combined with protein-RNA crosslinking. eLife 2017, 6, No. e29224. [PubMed: 29239719]

(23). Han S; et al. Proximity Biotinylation as a Method for Mapping Proteins Associated with mtDNA in Living Cells. Cell Chem. Biol 2017, 24, 404–414. [PubMed: 28238724]

(24). Chung CY; et al. In Situ Peroxidase Labeling and Mass-Spectrometry Connects Alpha-Synuclein Directly to Endocytic Trafficking and mRNA Metabolism in Neurons. Cell Syst 2017, 4, 242–250. [PubMed: 28131823]

(25). Navarrete-Perea J; Yu Q; Gygi SP; Paulo JA Streamlined Tandem Mass Tag (SL-TMT) Protocol: An Efficient Strategy for Quantitative (Phospho)proteome Profiling Using Tandem Mass Tag-Synchronous Precursor Selection-MS3. J. Proteome Res 2018, 17, 2226–2236. [PubMed: 29734811]

(26). Zhang T; Gygi SP; Paulo JA Temporal Proteomic Profiling of SH-SY5Y Differentiation with Retinoic Acid Using FAIMS and Real-Time Searching. J. Proteome Res 2021, 20, 704–714. [PubMed: 33054241]

(27). Perez-Riverol Y; et al. The PRIDE database and related tools and resources in 2019: improving support for quantification data. Nucleic Acids Res. 2019, 47, D442–D450. [PubMed: 30395289]

(28). Lam SS; et al. Directed evolution of APEX2 for electron microscopy and proximity labeling. Nat. Methods 2015, 12, 51–54. [PubMed: 25419960]

(29). Dong Y; et al. The cell surface glycoprotein CUB domain-containing protein 1 (CDCP1) contributes to epidermal growth factor receptor-mediated cell migration. J. Biol. Chem 2012, 287, 9792–9803. [PubMed: 22315226]

(30). Zehorai E; Yao Z; Plotnikov A; Seger R The subcellular localization of MEK and ERK—A novel nuclear translocation signal (NTS) paves a way to the nucleus. Mol. Cell. Endocrinol 2010, 314, 213–220. [PubMed: 19406201]

(31). Grumont RJ; Rasko JE; Strasser A; Gerondakis S Activation of the mitogen-activated protein kinase pathway induces transcription of the PAC-1 phosphatase gene. Mol. Cell. Biol 1996, 16, 2913–2921. [PubMed: 8649402]

(32). Brenner DA; O'Hara M; Angel P; Chojkier M; Karin M Prolonged activation of jun and collagenase genes by tumour necrosis factor-α. Nature 1989, 337, 661–663. [PubMed: 2537468]

(33). Devary Y; Gottlieb RA; Lau LF; Karin M Rapid and preferential activation of the c-jun gene during the mammalian UV response. Mol. Cell. Biol 1991, 11, 2804–2811. [PubMed: 1901948]

(34). Lin L-L; et al. cPLA2 is phosphorylated and activated by MAP kinase. Cell 1993, 72, 269–278. [PubMed: 8381049]

(35). Seger R; Krebs EG The MAPK signaling cascade. Faseb J. 1995, 9, 726–735. [PubMed: 7601337]

(36). Songyang Z; et al. A structural basis for substrate specificities of protein Ser/Thr kinases: primary sequence preference of casein kinases I and II, NIMA, phosphorylase kinase, calmodulin-dependent kinase II, CDK5, and Erk1. Mol. Cell. Biol 1996, 16, 6486–6493. [PubMed: 8887677]

(37). Al-Ayoubi AM; Zheng H; Liu Y; Bai T; Eblen ST Mitogen-Activated Protein Kinase Phosphorylation of Splicing Factor 45 (SPF45) Regulates SPF45 Alternative Splicing Site Utilization, Proliferation, and Cell Adhesion. Mol. Cell. Biol 2012, 32, 2880–2893. [PubMed: 22615491]

(38). Delghandi MP; Johannessen M; Moens U The cAMP signalling pathway activates CREB through PKA, p38 and MSK1 in NIH 3T3 cells. Cell Signal 2005, 17, 1343–1351. [PubMed: 16125054]

(39). Arora G; et al. Unveiling the novel dual specificity protein kinases in Bacillus anthracis: identification of the first prokaryotic dual specificity tyrosine phosphorylation-regulated kinase (DYRK)-like kinase. J. Biol. Chem 2012, 287, 26749–26763. [PubMed: 22711536]

(40). Schmidt PH; et al. AKAP350, a multiply spliced protein kinase A-anchoring protein associated with centrosomes. J. Biol. Chem 1999, 274, 3055–3066. [PubMed: 9915845]

(41). Schillace RV; Scott JD Association of the type 1 protein phosphatase PP1 with the A-kinase anchoring protein AKAP220. Curr. Biol 1999, 9, 321–324. [PubMed: 10209101]

(42). Wong W; Scott JD AKAP signalling complexes: focal points in space and time. Nat. Rev. Mol. Cell Biol 2004, 5, 959–970. [PubMed: 15573134]

(43). Pearson RB; Kemp BE Protein kinase phosphorylation site sequences and consensus specificity motifs: tabulations. Methods Enzymol 1991, 200, 62–81. [PubMed: 1956339]

(44). Montminy M Transcriptional regulation by cyclic AMP. Annu. Rev. Biochem 1997, 66, 807–822. [PubMed: 9242925]

(45). Law NC; Weck J; Kyriss B; Nilson JH; Hunzicker-Dunn M Lhcgr expression in granulosa cells: roles for PKA-phosphorylated beta-catenin, TCF3, and FOXO1. Mol. Endocrinol 2013, 27, 1295–1310. [PubMed: 23754802]

(46). Wang S; et al. Quantitative Phosphoproteomic Study Reveals that Protein Kinase A Regulates Neural Stem Cell Differentiation Through Phosphorylation of Catenin Beta-1 and Glycogen Synthase Kinase 3beta. Stem Cells 2016, 34, 2090–2101. [PubMed: 27097102]

(47). Ranieri A; Kemp E; Burgoyne JR; Avkiran M beta-Adrenergic regulation of cardiac type 2A protein phosphatase through phosphorylation of regulatory subunit B56delta at S573. J. Mol. Cell Cardiol 2018, 115, 20–31. [PubMed: 29294329]

(48). Carlson SM; White FM Expanding applications of chemical genetics in signal transduction. Cell Cycle 2012, 11, 1903–1909. [PubMed: 22544320]

(49). Vinciguerra M; et al. Differential Phosphorylation of c-Jun and JunD in Response to the Epidermal Growth Factor Is Determined by the Structure of MAPK Targeting Sequences. J. Biol. Chem 2004, 279, 9634–9641. [PubMed: 14676207]

(50). Sears R; et al. Multiple Ras-dependent phosphorylation pathways regulate Myc protein stability. Genes Dev. 2000, 14, 2501–2514. [PubMed: 11018017]

(51). Pulverer BJ; et al. Site-specific modulation of c-Myc cotransformation by residues phosphorylated in vivo. Oncogene 1994, 9, 59–70. [PubMed: 8302604]

(52). Honig A; Auboeuf D; Parker MM; O'Malley BW; Berget SM Regulation of alternative splicing by the ATP-dependent DEAD-box RNA helicase p72. Mol. Cell. Biol. 2002, 22, 5698–5707. [PubMed: 12138182]

(53). Dardenne E; et al. Splicing switch of an epigenetic regulator by RNA helicases promotes tumor-cell invasiveness. Nat. Struct Mol. Biol 2012, 19, 1139–1146. [PubMed: 23022728]

(54). Niinae T; Imami K; Sugiyama N; Ishihama Y Identification of Endogenous Kinase Substrates by Proximity Labeling Combined with Kinase Perturbation and Phosphorylation Motifs. Mol. Cell Proteomics 2021, 20, 100119. [PubMed: 34186244]

(55). Huttlin EL; et al. Dual proteome-scale networks reveal cell-specific remodeling of the human interactome. Cell 2021, 184, 3022–3040. [PubMed: 33961781]

(56). Sudakin V; Chan GK; Yen TJ Checkpoint inhibition of the APC/C in HeLa cells is mediated by a complex of BUBR1, BUB3, CDC20, and MAD2. J. Cell Biol 2001, 154, 925–936. [PubMed: 11535616]

(57). Li Y; Benezra R Identification of a Human Mitotic Checkpoint Gene: hsMAD2. Science 1996, 274, 246–248. [PubMed: 8824189]

(58). Zhang Y; Lees E Identification of an overlapping binding domain on Cdc20 for Mad2 and anaphase-promoting complex: model for spindle checkpoint regulation. Mol. Cell. Biol 2001, 21, 5190–5199. [PubMed: 11438673]

(59). Li J; et al. TMTpro-18plex: The Expanded and Complete Set of TMTpro Reagents for Sample Multiplexing. J. Proteome Res 2021, 20, 2964–2972. [PubMed: 33900084]

(60). Li J; et al. TMTpro reagents: a set of isobaric labeling mass tags enables simultaneous proteome-wide measurements across 16 samples. Nat. Methods 2020, 17, 399–404. [PubMed: 32203386]

(61). Rhee SG Cell signaling. H2O2, a necessary evil for cell signaling. Science 2006, 312, 1882–1883. [PubMed: 16809515]

(62). Lopez MS; Kliegman JI; Shokat KM The logic and design of analog-sensitive kinases and their small molecule inhibitors. Methods Enzymol 2014, 548, 189–213. [PubMed: 25399647]

(63). Schweppe DK; et al. Characterization and Optimization of Multiplexed Quantitative Analyses Using High-Field Asymmetric-Waveform Ion Mobility Mass Spectrometry. Anal. Chem 2019, 91, 4010–4016. [PubMed: 30672687]

(64). Schweppe DK; et al. Full-Featured, Real-Time Database Searching Platform Enables Fast and Accurate Multiplexed Quantitative Proteomics. J. Proteome Res. 2020, 19, 2026–2034. [PubMed: 32126768]

(65). Paul S; et al. Activation-induced substrate engagement in ERK signaling. Mol. Biol. Cell 2020, 31, 235–243. [PubMed: 31913744]

(66). Giansanti P; Stokes MP; Silva JC; Scholten A; Heck AJ Interrogating cAMP-dependent kinase signaling in Jurkat T cells via a protein kinase A targeted immune-precipitation phosphoproteomics approach. Mol. Cell Proteomics 2013, 12, 3350–3359. [PubMed: 23882029]

(67). Su YH; Chen SH; Zhou H; Vacquier VD Tandem mass spectrometry identifies proteins phosphorylated by cyclic AMP-dependent protein kinase when sea urchin sperm undergo the acrosome reaction. Dev. Biol 2005, 285, 116–125. [PubMed: 16038896]

(68). Neukamm SS; et al. Phosphorylation of serine 1137/1138 of mouse insulin receptor substrate (IRS) 2 regulates cAMP-dependent binding to 14–3-3 proteins and IRS2 protein degradation. J. Biol. Chem 2013, 288, 16403–16415. [PubMed: 23615913]

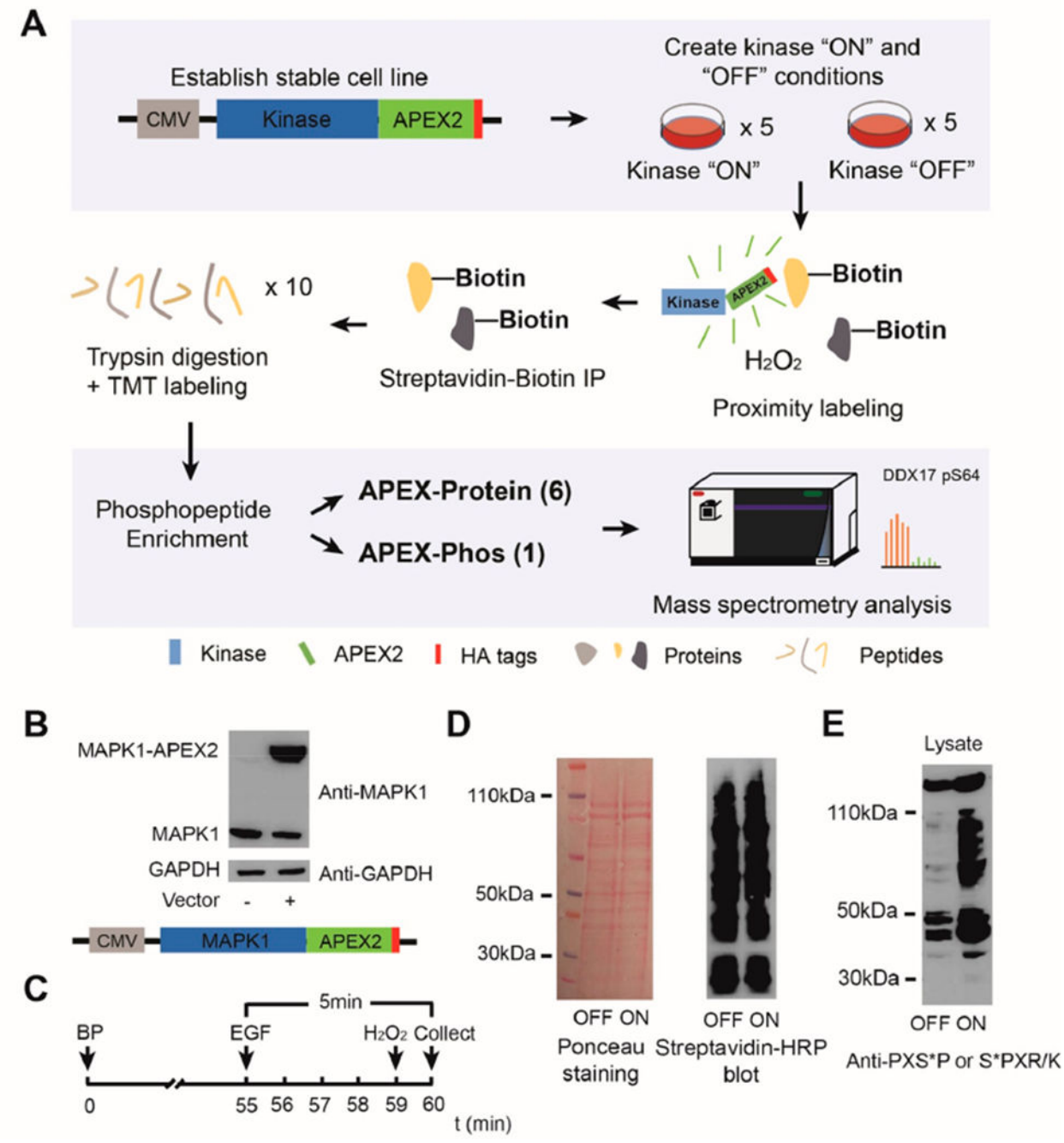

Figure 1.

Phospho-APEX (pAPEX) enriches proteins in close proximity to APEX2 tagged kinase. (A) Workflow of a pAPEX experiment. Cells are engineered to stably express the targeted kinase with an APEX2 tag and 3× HA epitope tags. Proximity labeling is performed under the kinase "OFF" and kinase "ON" conditions with replicates. During 1 min of H_2O_2 treatment, APEX2 catalyzes the transfer of biotin phenol (BP) to proteins surroundings the APEX2 fused protein radius (1–10 nm). In a typical TMT-10plex experiment, five replicates of cells under the kinase "ON" and "OFF" conditions are used to improve the statistical

power. Biotinylated proteins are pulled down by streptavidin immunoprecipitation, digested, TMT-labeled, and combined prior to phosphopeptide enrichment. The flow-through of the phosphopeptide enrichment is fractionated into six fractions, which we refer to as APEX-Protein. The phosphopeptide fraction and six fractions of APEX-Protein are analyzed using mass spectrometry with reporter ion quantification. Comparing phosphopeptide abundance changes for the kinase “ON” and “OFF” conditions can reveal candidate kinase substrates. (B) Western blotting analysis showing the stable expression of the MAPK1-APEX2 fusion protein in HEK293T cells. (C) Time course of the proximity labeling experiment under the kinase “ON” condition in MAPK1-pAPEX experiment. (D) Biotinylated proteins from the proximity labeling experiment in HEK293T cells were analyzed by Ponceau staining (left) and streptavidin-HRP Western blotting (right). (E) Western blotting analysis using antibodies recognizing the consensus motif for MAPK phosphorylation.

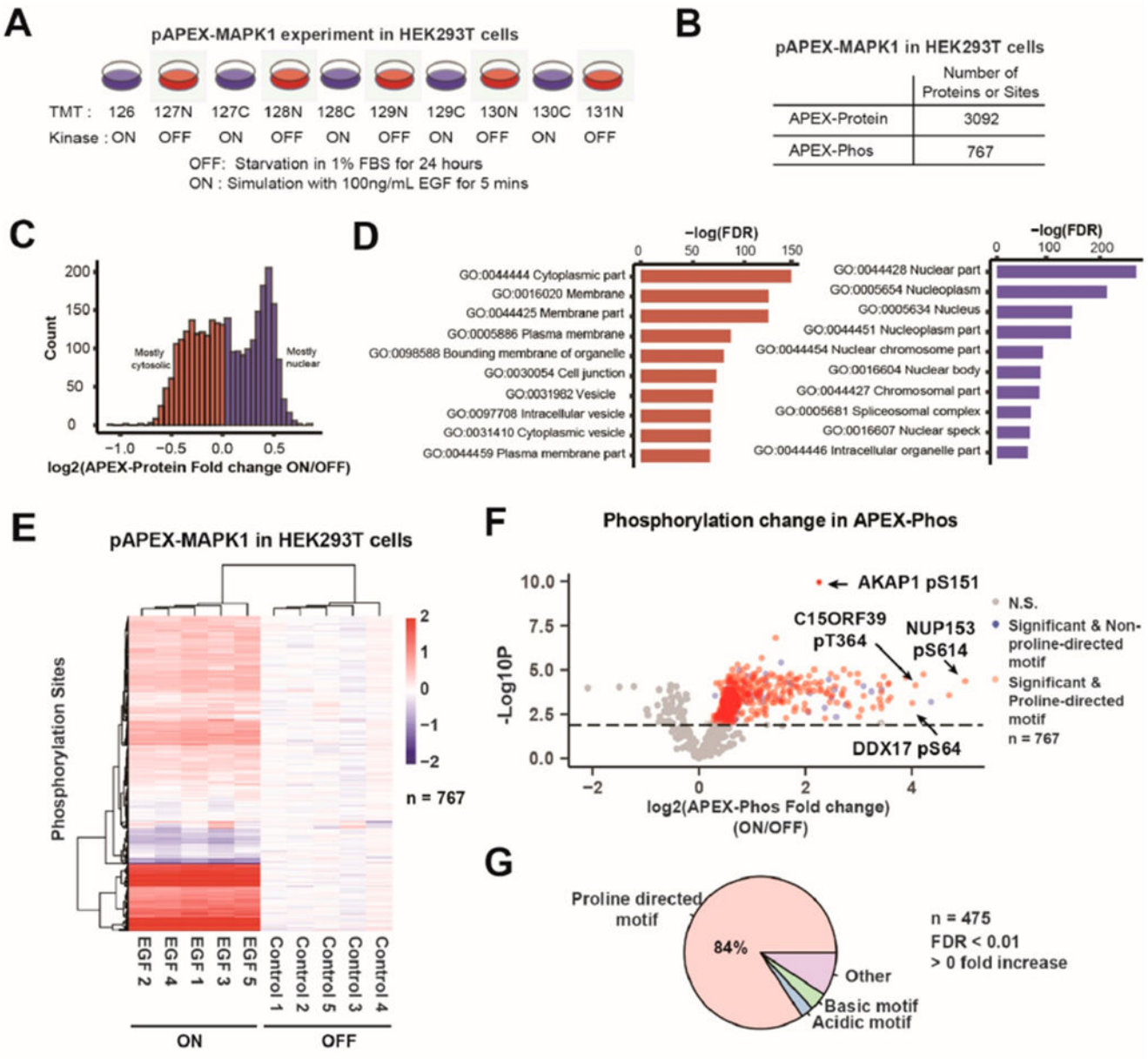

Figure 2.

pAPEX quantified proteins and phosphorylated peptides in close proximity to APEX2 tagged MAPK1 in HEK293T cells. (A) Experimental overview. (B) Proteins and sites identified. (C) Biotinylated proteins are highly enriched in nuclear proteins after 5 min EGF treatment, suggesting relocalization of MAPK1. (D) Gene ontology enrichment categories for proteins quantified in APEX-Protein analysis using proteins highlighted in red or blue in Panel C. Heatmap (E) and volcano plot (F) of phosphorylation sites quantified. In the heatmap, $\log_2$(ON/OFF) ratios were calculated and plotted; the five control and five EGF-treated samples clustered. In the volcano plot, sites are colored based on significance and whether or not they contained a proline-directed motif. (G) Pie chart of the significant (colored) sites in Panel F. The majority (84%) of sites were classified as proline-directed.

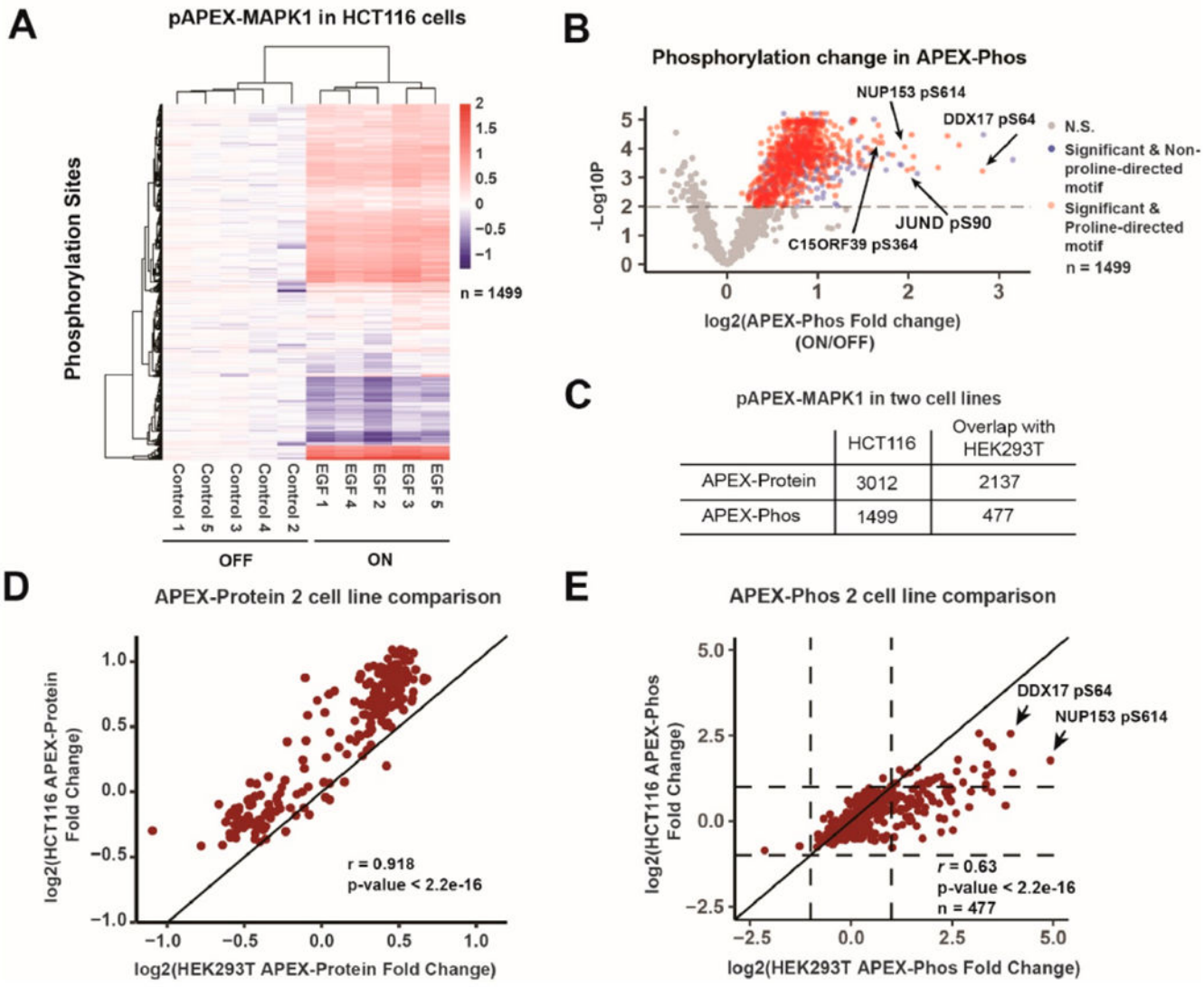

Figure 3.

APEX quantified proteins and phosphorylated peptides in close proximity to APEX2 tagged MAPK1 in HCT116 cells. The experiment shown in Figure 2A was repeated in HCT116 cells. Heatmap (A) and volcano plot (B) of phosphorylation sites quantified in pAPEX-MAPK1 in HCT116 cells. (C) Comparison of proteins and phosphorylation sites quantified in the two cell lines. (D) Scatterplot of the APEX-Protein change in the two cell lines (r = 0.918). The unity line is drawn. (E) Scatterplot of APEX-Phos changes in the two cell lines (r = 0.63). HEK293T cells are more responsive on average to EGF treatment than HCT116 cells which harbor the $KRAS^{G12D}$ allele already activating the MAPK pathway. The unity line is drawn. Dashed vertical and horizontal lines represent 0 (no change) and 1 (2-fold change). pS614 of NUP153 and pS64 of DDX17 are indicated.

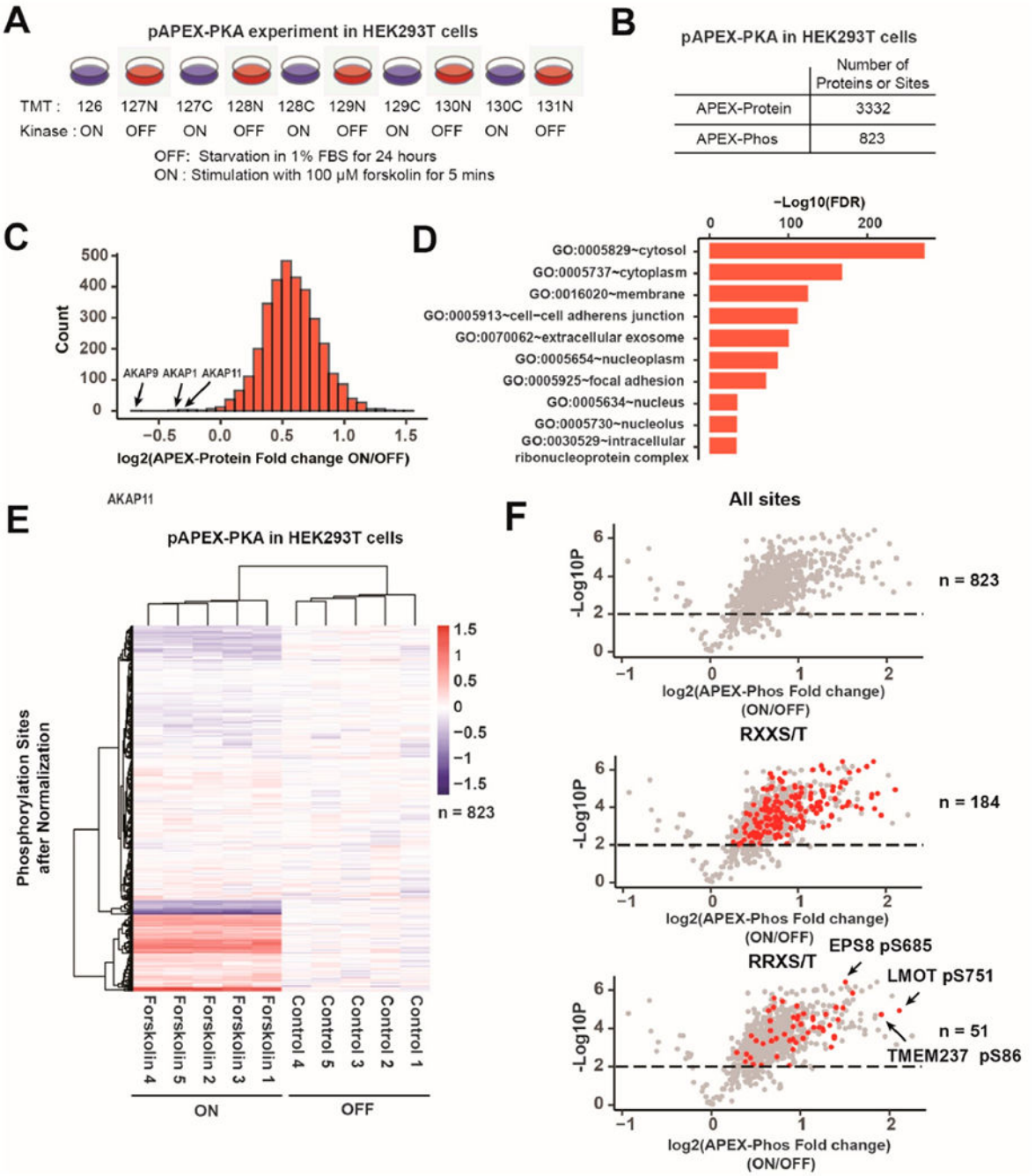

Figure 4.

pAPEX quantified proteins and phosphorylated peptides in close proximity to APEX2 tagged PKA in HEK293T cells. (A) Experimental overview. (B) Quantified proteins and sites. (C) Distribution of log2(fold change ON/OFF) for proteins quantified in the APEX-Protein. (D) Gene ontology enrichment categories for all proteins quantified in the APEX-Protein analysis. (E) Heatmap of phosphorylation sites quantified. Log2(fold change (ON/OFF)) were calculated and plotted. The five control and five forskolin treated samples

clustered. (F) Volcano plots of quantified phosphorylation events. Sites with significant changes are colored based on site's underlying motif (RXXS/T or RRXS/T).

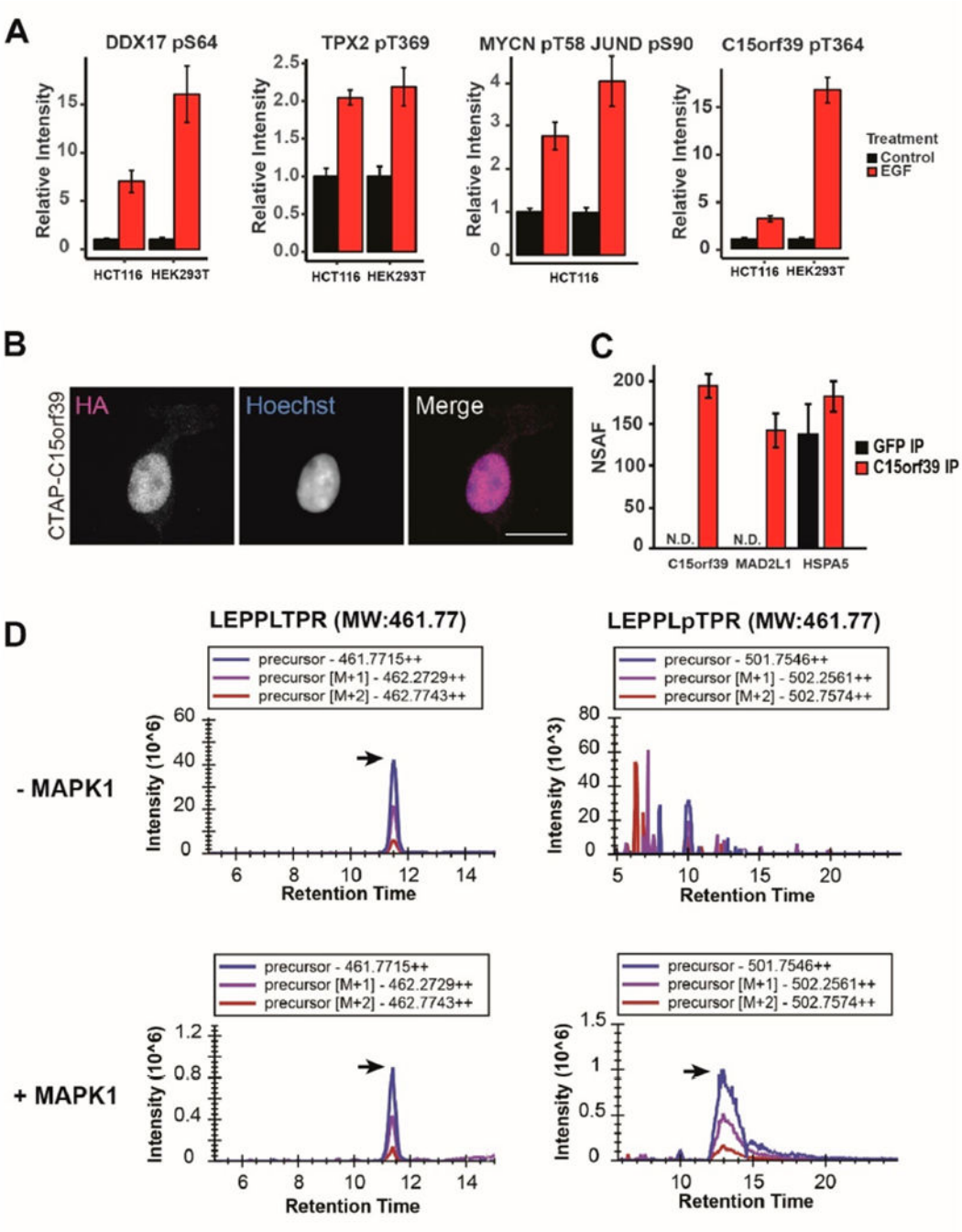

Figure 5.

C15orf39 can be phosphorylated by MAPK1 in vitro. (A) Phosphorylation levels for several sites in two different cell lines. T364 from C15orf39 increased in both HCT116 and HEK293T cells after EGF treatment. (B) Epitope-tagged C15orf39 localizes to the nucleus. HEK293T cells stably expressing C-terminal FLAG-HA tagged (CTAP) C15orf39 were fixed and stained with anti-HA antibodies to visualize ectopic protein localization via confocal microscopy. Max intensity projections of 2 μm z-stacks are shown; scale bar represents 20 μm. (C) HA immunoprecipitation of C15orf39 specifically enriched MAD2L1

as a candidate binding partner. HSPA5 is shown as a background control. (D) *In vitro* kinase assay using MAPK1 and purified C15orf39 protein. After incubation with ATP and MAPK1, C15orf39 showed increased abundance of the phosphorylated form of LEPPLpTPR and decreased signal for the nonphosphorylated form (LEPPLTPR). Base peak chromatograms using isotopic envelope peaks were visualized in Skyline.

Table 1.

Examples of Candidate Substrates[a] of MAPK1 Identified in the pAPEX-MAPK1 Experiment in HCT116 and HEK293T Cells

Gene Symbol	Motif Sequence	Site Position	(EGF/Control) HCT116	(EGF/Control) HEK293T	References
POLA1	**RKEPPLTPVPLKR**	219	10.7	16.6	-
RBFOX2	**MQNEPLTPGYHGF**	67	3.3	6.8	-
RPRD2	**QKQYPDSPHPVPH**	965	6.5	9.7	-
C15orf39	**KLEPPLTPRCPLD**	364	16.8	20.0	-
FOXK2	**AQSAPGSPLSSQP**	428	2.8	6.0	-
TPX2	**PLTVPVSPKFSTR**	738	4.5	7.3	48
ARID1B	**PAMSPGTPGPTMG**	505	4.2	6.9	-
SFPQ	**RGMGPGTPAGYGR**	687	4.0	6.5	-
USF2	**PRTHPYSPKIDGT**	222	2.2	4.8	-
CIC	**EPPTPPSPAPAPA**	2201	5.5	7.8	65

[a]Among the identified MAPK1 candidate substrates in both HCT116 cells and HEK293T cells, 99 sites contained the PXS/TP motif. Ten example sites are shown here.

Table 2.

Examples of Candidate Substrates[a] of PKA Identified in the pAPEX-PKA Experiment in HEK293T Cells

Gene Symbol	Motif Sequence	Site Position	Fold Change (Forskolin/Control)	References
LMO7	**WKDRRKSYTSDLQ**	751	4.3	66
TMEM237	**TAGRRPSEGNEPS**	86	3.8	-
EPS8	**PVDRRKSQMEEVQ**	685	3.0	67
CASC5	**KNSRRVSFADTIK**	60	2.8	66
CTNNB1	**DTQRRTSMGGTQQ**	552	2.8	45
CCDC88C	**LDTRRFSLAPPKE**	1887	2.7	-
LUZP1	**ASSRRSSSEGLSK**	574	2.6	66
IRS2	**RSYRRVSGDAAQD**	560	2.6	68
PPP2R5D	**VLLRRKSELPQDV**	573	2.5	47
RAB11FIP1	**PESRRSSLLSLMT**	435	2.5	-

[a]Among the identified PKA candidate substrates in HEK293T cells, 46 sites contained the RRXS/T motif. Ten example sites are shown here.